J Neurophysiol 130: 1444–1456, 2023.
First published November 15, 2023; doi:10.1152/jn.00091.2023

american physiological society

JNP JOURNAL OF NEUROPHYSIOLOGY

RESEARCH ARTICLE

Control of Movement

A table tennis serve versus rally hit elicits differential hemispheric electrocortical power fluctuations

Amanda Studnicki,[1] Rachael D. Seidler,[2] and Daniel P. Ferris[1]

[1]*J. Crayton Pruitt Family Department of Biomedical Engineering, University of Florida, Gainesville, Florida, United States and*
[2]*Department of Applied Physiology & Kinesiology, University of Florida, Gainesville, Florida, United States*

Abstract

Human visuomotor control requires coordinated interhemispheric interactions to exploit the brain's functional lateralization. In right-handed individuals, the left hemisphere (right arm) is better for dynamic control and the right hemisphere (left arm) is better for impedance control. Table tennis is a game that requires precise movements of the paddle, whole body coordination, and cognitive engagement, providing an ecologically valid way to study visuomotor integration. The sport has many different types of strokes (e.g., serve, return, and rally shots), which should provide unique cortical dynamics given differences in the sensorimotor demands. The goal of this study was to determine the hemispheric specialization of table tennis serving – a sequential, self-paced, bimanual maneuver. We used time-frequency analysis, event-related potentials, and functional connectivity measures of source-localized electrocortical clusters and compared serves with other types of shots, which varied in the types of movement required, attentional focus, and other task demands. We found greater alpha (8–12 Hz) and beta (13–30 Hz) power in the right sensorimotor cortex than in the left sensorimotor cortex, and we found a greater magnitude of spectral power fluctuations in the right sensorimotor cortex for serve hits than return or rally hits, in all right-handed participants. Surprisingly, we did not find a difference in interhemispheric functional connectivity between a table tennis serve and return or rally hits, even though a serve could arguably be a more complex maneuver. Studying real-world brain dynamics of table tennis provides insight into bilateral sensorimotor integration.

NEW & NOTEWORTHY We found different spectral power fluctuations in the left and right sensorimotor cortices during table tennis serves, returns, and rallies. Our findings contribute to the basic science understanding of hemispheric specialization in a real-world context.

electroencephalography; interhemispheric interaction; table tennis

INTRODUCTION

Hemispheric specialization has a long history of research and is thought to be an important factor in the organization and function of the brain (1–5). In visuomotor control, the left hemisphere is associated with higher-order aspects of coordination such as skilled movement and language (6–8), whereas the right hemisphere is involved in global features of visuospatial processing (9, 10). Effective interhemispheric integration is vital for coordinated, everyday movements.

Traditional neuroimaging studies have been limited to simple laboratory-based tasks due to technological constraints. Functional magnetic resonance imaging (fMRI) and positron emission tomography (PET) scans require participants to remain stationary inside big machines. Electroencephalography (EEG) offers high temporal resolution, on the scale of milliseconds, and easier portability than fMRI or PET, but EEG has traditionally been constrained to stationary tasks due to movement artifacts. However, recent advances in hardware and software have enabled mobile EEG studies (11–13). A previous analysis from our laboratory demonstrated the feasibility of recording high-fidelity EEG data during table tennis (14).

A table tennis serve is a complex, sequential, self-paced movement that could be used to study the visuomotor control of a real-world, complex maneuver (15). Right-handed

Correspondence: A. Studnicki (amandastudnicki@gmail.com).
Submitted 1 March 2023 / Revised 10 October 2023 / Accepted 8 November 2023

players toss the ball with their left hand and hit the ball with a paddle in their right hand. A successful serve requires bimanual coordination and likely activates bilateral sensorimotor networks in the brain (16). The serve is the only shot that uses both hands to manipulate the ball and paddle, unlike return and rally hits that use one hand to intercept an incoming ball.

In this study, we sought to determine the hemispheric specialization for an ecologically valid, sequential, bimanual task (e.g., a table tennis serve). Our aim was to investigate whether the left or right sensorimotor cortices showed a greater magnitude of spectral power fluctuations during a table tennis serve. To do this, we performed time-frequency analysis on source-localized EEG sensorimotor clusters from participants playing table tennis. As a means of contrast, we compared serve hits to other types of table tennis hits such as the return of serve and rally hits. Each type of shot varied in the movements required, attentional focus, and other task demands – all of which have been shown to affect hemispheric bias (2).

We hypothesized that serve hits would show a greater magnitude of spectral power fluctuations across the entire swing in the right sensorimotor cortex than return or rally hits. Event-related desynchronization (ERD) often occurs during motor planning and execution, and event-related synchronization (ERS) typically follows movement termination (i.e., the beta rebound) (17, 18). Dynamic changes in power indicate an increased involvement of that brain area for the experimental task (19). We believed that serve hits would require more involvement of the right sensorimotor cortex because the serve is the only shot in table tennis that uses the left hand to toss the ball (for right-handed participants). Given that the brain controls movement (largely) contralaterally (20), we predicted that serving the ball would show an increased involvement of the right sensorimotor cortex to control the left-handed toss.

We also hypothesized that functional connectivity would be higher between the left and right hemispheres for a serve than for rally or return hits. Asynchronous, temporally coordinated bimanual maneuvers require more bilateral brain activation, less interhemispheric inhibition, and more communication between the two hemispheres than unimanual maneuvers in healthy young adults (21–28). Previous studies used simple finger-tapping tasks to study bimanual coordination (26, 29, 30). However, everyday life is filled with bimanual activities that are more complex than finger movements. Studying the visuomotor control of table tennis serve could provide valuable insights into the neural mechanisms underlying the execution and control of real-world, self-paced movements. This information could have practical applications in fields such as sports training and rehabilitation, where improving bimanual visuomotor skills is important for performance and functional recovery.

METHODS

Participants

Thirty-seven participants (ages 23.5 ± 6.7 yr, 13 females) enrolled in our study. All participants were right-handed, self-reported as being fit to play, had normal or corrected-to-normal vision, and were skilled enough to repeatedly make contact with the ball. Our protocol was approved by the University of Florida Institutional Review Board, and we obtained written informed consent from each participant.

Experimental Design and Procedure

Our analysis used a table tennis data set reported in a previous study (14). Participants played in a variety of table tennis trials separated into four blocks of 15 min. Within each block, half of the trials were with a human player and the other half were with a ball machine. For this analysis, we focused on the human player trials only. The participants played either competitively or cooperatively for a continuous 7.5 min. Participants were instructed to try winning a 21-point game in the competitive trials, switching serves every five points. In the cooperative trials, we instructed participants to work together with the human player to keep the ball in play as long as possible. The human player (A.S.) was experienced and scaled their play to the level of the participant. We collected a 5-min standing baseline at the beginning and end of the experiment, totaling 70 min of data collection (not including breaks).

Data Acquisition

We collected dual-layer EEG (14, 31) data from 120 scalps and 120 noise electrodes logged on four LiveAmp 64 amplifiers (BrainVision ActiCAP, 500 Hz). Eight of the 128 original scalp electrodes near the back of the head were re-purposed to measure neck muscle activity. We separated the online reference (CPz) and online ground (Fpz) for the scalp and noise layers, as recommended for the dual-layer EEG setup (31). Before the start of the experiment, we acquired a three-dimensional (3-D) head scan of the electrode locations using itSeez3D software (Structure Sensor from Occipital Inc.). We recorded the timing of hit events using the acceleration from inertial measurement units (IMU) on the handles of two wooden paddles (Cometa WaveTrack Inertial System, 2,000 Hz). Hits were defined when the first derivative of the resultant acceleration exceeded 0.75 gravity. We also recorded video (GoPro Hero 7, range of 30–240 fps) of all the trials, which helped in postprocessing to filter out any mislabeled events. The EEG and inertial measurement unit data were synchronized using pulses from an Arduino every 5 s, and the video was aligned to the data using a cross-correlation between the IMU acceleration and the timing of hits that were manually marked in Adobe Premiere Pro software. Any inertial measurement unit hit events outside of 200 ms from the video markers were removed. On a different day, we collected a T1 structural MRI scan of the participants' head (3 T Philips Ingenia Scanner) using a 32-channel head coil. Sixteen participants were scanned with 7.00 ms repetition time, 3.17 ms echo time, 8° flip angle, 240 × 240 × 176 mm field of view, and 1 mm^3 recon voxel size. Twenty-one participants were scanned with 11.13 repetition time, 5.10 ms echo time, 8° flip angle, 256 × 240 × 179.9 mm field of view, and 0.67 × 0.67 × 0.67 mm^3 recon voxel size.

Data Processing

We processed data using custom scripts (MATLAB, R2020A) and open-source software such as EEGLAB v2021.0, FieldTrip,

and Computational Anatomy Toolbox for SPM (CAT12.8). Data were 1 Hz high-pass filtered to remove drift. We marked hit events, visually inspected, and manually separated trials into individual datasets based on continuous blocks of hit events. We removed 60 Hz line noise with Cleanline (32), downsampled the data to 250 Hz, rejected bad channels that were outside of three standard deviations from the median of other channels, averaged re-referenced the data with full rank, and spherically interpolated the rejected channels. We used iCanClean (33, 34) to address motion and muscle artifacts (2-s sliding window). We used an r^2 threshold of 0.85 to reject subspaces of scalp electrodes that correlated with the noise electrodes and an r^2 threshold of 0.40 to reject subspaces of scalp electrodes that correlated with the muscle channels. Then, we used clean_artifacts to perform time window rejection with a standard deviation threshold of 30 and a window criterion of 0.3.

To minimize the effects of volume conduction on subsequent analyses, we used an Independent component analysis (ICA) based approach (35). First, principal component analysis reduced the number of principal components by the maximum number of scalp channels that were interpolated across trials for each participant. Then, we ran adaptive mixture independent component analysis (AMICA) to separate the signal into maximally temporally independent components (36, 37). We applied the resulting weight matrix to the data before the time window rejection.

We created participant-specific conduction head models with the finite element method in the FieldTrip-SimBio pipeline (38). We marked the electrode locations on the 3-D head scan using EEGLAB get_chanlocs and specified an inward shift of 10 mm to account for the extra height of the dual-layer electrodes. The participant's T1 MR images were segmented into five tissue layers using the CAT12 plug-in for SPM, and tissue connectivity values were specified according to Ref. 39 (skin: 430, skull: 10, CSF: 1,790, gray matter: 330, white matter: 140 mS/m). Then, we meshed the tissues into hexahedrons, aligned the head model with the electrode locations based on fiducials (nasion and left/right preauricular points), and computed the source model, transfer matrix, and leadfield matrix with FieldTrip functions.

DIPFIT 3.3 allowed us to fit each independent component to an equivalent dipole to our custom head models. We converted the dipole locations to Montreal Neurological Institute (MNI) space and retained components that explained more than 85% of the scalp variance (35, 40). With a combination of ICLabel and visual inspection (41, 42), we only chose brain components for further analysis and then clustered the remaining brain components using k-means by dipole location. We chose $k = 10$ clusters based on the silhouette algorithm (43) and assigned any dipoles more than three standard deviations from the cluster centroids as outliers. Clusters with components from more than 50% of the participants were further analyzed. If more than one component per participant contributed to a cluster, we retained the component with the lowest residual variance. We removed an average of nine components per cluster.

We performed a secondary analysis at the electrode-level, instead of the component-level, which follows the approach of more traditional EEG studies. The preprocessing remained the same, except we used more conservative criteria for component selection after independent component analysis. We rejected components that were more than 75% labeled as non-brain by ICLabel. Then, we back-projected the components and focused on channels F3 and F4 (an equivalent to left/right cingulate), C3 and C4 (an equivalent to left/right sensorimotor), and P3 and P4 (an equivalent to left/right parietal).

There were three different hit types in our analyses: rally, return, and serve hits (Fig. 1). Both return and serve hits occurred at the beginning of the point (competitive trials) or friendly volley (cooperative trials). The rally hits were the subsequent shots that occurred after the point started. A serve hit was the only shot that required bimanual coordination – tossing the ball with the left hand and hitting the ball with the paddle in the right hand. Data were epoched −1.5 to 1.5 s around when the participant's paddle made contact with the ball (*time 0*). We rejected 10% of the epochs that had the highest voltage maxima to get rid of noisy epochs. Since there were fewer serve hits than other rally and return hits, we randomly sampled the epochs to the average number of serve hits across participants (50 epochs).

Outcome Measures

We calculated the average EEG log spectral power density (PSD) to measure any total power differences between the left and right hemispheres in the cingulate gyrus, sensorimotor, and parietal cortices. The spectopo function in EEGLAB gave us individual power spectral densities (nonoverlapping hamming windows with the pwelch method, 250 window length). Then, we used the FOOOF toolbox to model the power spectra from 3 to 40 Hz, peak width limits [1 Hz, 8 Hz], minimum peak height of 0.05, and maximum number of peaks being 2. This allowed us to compute flattened power spectra by removing the aperiodic components from the original power spectra. We tested for significant differences in alpha/mu (8–12 Hz) and beta (13–30 Hz) power between the left and right sensorimotor cortex for each of the hit types using a two-way repeated-measures ANOVA for participants that contributed a component to both clusters ($n = 11$).

We performed time-frequency analysis and calculated single trial spectrograms using newtimef. We took the mean event-related spectral perturbation (ERSP) across components in each cluster to create a grand average ERSP. The spectral baseline was the average power in the epoch for all hit types. We bootstrapped individual ERSPs (0.05 alpha, 2,000 iterations) to find statistically significant time-frequency changes within each hit type and corrected for multiple comparisons using the false discovery correction with the Benjamini and Hochberg method (44). Nonsignificant values were set to zero. We used nonparametric statistics with cluster-based multiple comparison corrections to compute significance-masked difference ERSPs (Serve–Rally, Serve–Return, and Return–Rally) (45).

We also compared the left and right sensorimotor clusters by subtracting a spectral baseline that was the average power in the epoch across the two clusters. Then, we focused on the alpha (8–12 Hz) and beta (13–30 Hz) frequency bands by averaging the power in those bands to plot the change in power across time. Significant differences in power between left and right sensorimotor cortices were tested with a two-sided Wilcoxon signed rank test in four separate time windows (−1,000 to −500 ms,−500 to 0 ms, 0 to 500 ms, and 500 to 1,000 ms around the hit event).

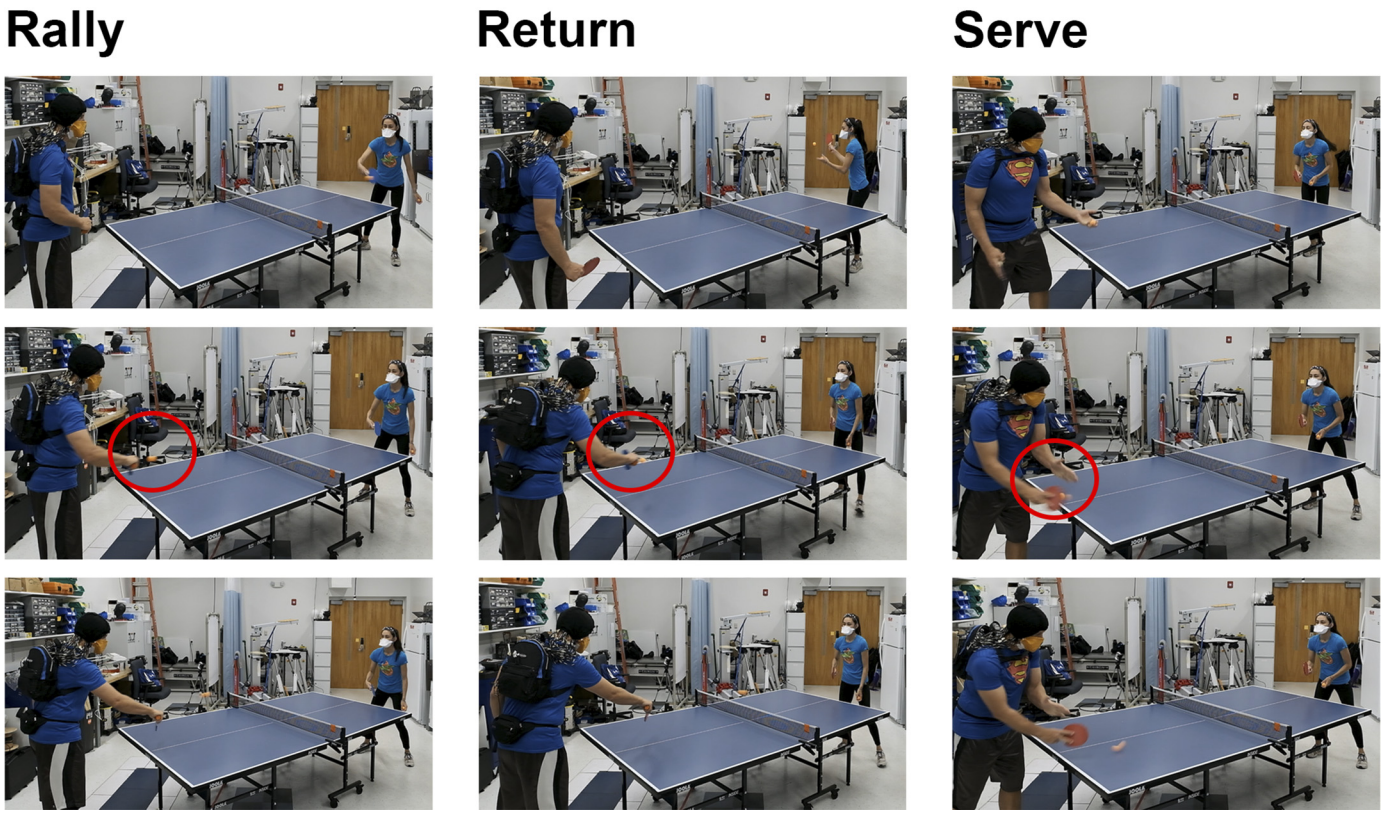

Figure 1. Rally, return, and serve hits. In a rally, the participant (*left* side of each picture) played table tennis in a continuous volley of hits with the human player (*right* side of each picture). In a return, the rally had not started yet, and the participant prepared to return the serve from the human player. In a serve, the participant began the rally by tossing the ball with their left hand and hitting the ball with the paddle in their right hand. Epochs for subsequent analyses were centered on the participant hit (*time 0*, circled in red).

Event-related potentials (ERPs) and intertrial phase coherence (ITPC) measured the consistency of phase across trials within a cluster. We averaged the event-related potentials across participants. For the intertrial phase coherence, we found the mean across participants in each cluster, bootstrapped individual ITPCs (0.05 alpha, 2,000 iterations), and masked for significance at 0.05 alpha (corrected for multiple comparisons with the Benjamini and Hochberg false discovery rate correction). We used nonparametric statistics with cluster-based multiple comparison corrections for the different ERSPs. According to Ref. 46, researchers must be careful to draw conclusions from small changes in ITPC. Therefore, we chose a conservative approach and additionally set any values less than 0.1 ITPC to zero.

Event-related phase coherence (ERCOH) gave us a measure of functional connectivity between the source-localized clusters (47). For each calculation, we only included participants who contributed a component to both clusters for each pairwise comparison. We used the function newcrossf with epoch latency limits −0.5 to 1.0 s around the hit event, averaged the coherence across participants, bootstrapped individual ERCOH spectrograms, and masked for significance at 0.05 alpha (2,000 iterations, shuffled along the time dimension). Nonparametric permutation statistics with cluster-based multiple comparison corrections (2,000 iterations, 0.05 alpha) assessed the significant differences across the hit types.

Accessibility

Raw and processed data files can be accessed at doi.org/10.18112/openneuro.ds004505.v1.0.4. The data have been organized according to the BIDS standard (48, 49).

RESULTS

The resulting clusters that contained components from more than half of the participants were found in the left and right cingulate gyrus, left and right sensorimotor, supplementary motor area, precuneus, cuneus, and left and right parieto-occipital cortices (Fig. 2). MNI coordinates of the cluster centroids are shown in Table 1.

Cortical clusters had increased power in the theta (3–8 Hz), alpha (8–12 Hz), and beta (13–30 Hz) bands above the aperiodic component (Fig. 3). When comparing the shape of the power spectral density plots between left and right hemispheres, the left/right cingulate and left/right parieto-occipital brain areas were very similar, whereas there were notable differences in power between the left and right sensorimotor cortices. The 2 × 3, two-way, repeated-measures ANOVA of the flattened alpha power with hemisphere (left and right) and hit type (rally, return, and serve) as within-subjects factors revealed a main effect of hemisphere, $F(1, 60) = 10.81$, $P = 0.0017$. There was no main effect of hit type, $F(2, 60) = 0.34$, $P = 0.7156$. There were no significant interactions between hemisphere and hit type, $F(2, 60) = 0.03$, $P =$

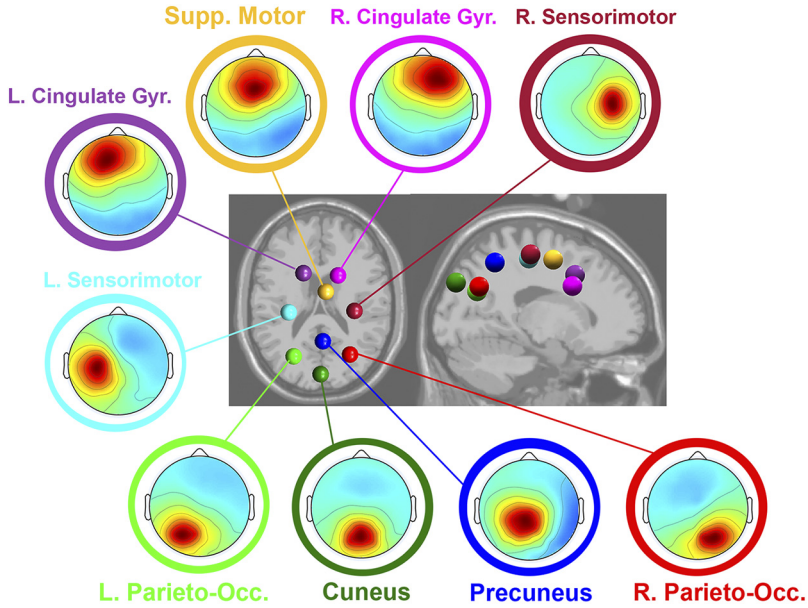

Figure 2. Cluster centroids and corresponding group-average component scalp maps for the nine clusters that contained dipoles from more than half of the participants: right sensorimotor (dark red, 13 participants), right cingulate gyrus (magenta, 18 participants), supplementary motor area (yellow, 15 participants), left cingulate gyrus (purple, 18 participants), left sensorimotor (cyan, 17 participants), left parieto-occipital (light green, 18 participants), cuneus (dark green, 16 participants), precuneus (dark blue, 21 participants), and right parieto-occipital (light red, 19 participants).

0.9658. The two-way ANOVA of the flattened beta power revealed a main effect of the hemisphere, $F(1, 60) = 6.22$, $P = 0.0154$. There was no main effect of hit type, $F(2, 60) = 0.73$, $P = 0.4875$. There were no significant interactions between hemisphere and hit type, $F(2, 60) = 1.34$, $P = 0.2702$. The average power of the left and right sensorimotor clusters in the alpha and beta bands are summarized in Fig. 4.

In the channel-level analysis, we found small increases in power in the theta (3–8 Hz), alpha (8–12 Hz), and gamma (30+ Hz) bands above the aperiodic component with little difference between the electrodes over the left or right hemisphere (Supplemental Fig. S1). The repeated-measures ANOVA of the flattened alpha power with channel (C3 left and C4 right) and hit type (rally, return, and serve) as within-subjects factors revealed no significance for hemisphere: $F(1, 144) = 1.76$, $P = 0.1872$, no significance for hit type: $F(2, 144) = 1.27$, $P = 0.2847$, and no significant interaction: $F(2, 144) = 0.02$, $P = 0.9789$. The repeated-measures ANOVA of the flattened beta power revealed no significance for hemisphere: $F(1, 144) = 0.14$, $P = 0.7102$, no significance for hit type: $F(2, 144) = 1.16$, $P = 0.3177$, and no significant interaction between hemisphere and hit type: $F(2, 144) = 0.4$, $P = 0.6692$. The average power of the channels C3 and C4 in the alpha and beta bands are summarized in Supplemental Fig. S2.

Table 1. *Coordinates of the cluster centroids in MNI space*

Cluster	MNI Coordinates
Right sensorimotor	34, −24, 57
Right cingulate gyrus	18, 11, 31
Supplementary motor area	6, −5, 53
Left cingulate gyrus	−16, 13, 40
Left sensorimotor	−31, −25, 54
Left parieto-occipital	−26, −68, 27
Cuneus	0, −86, 34
Precuneus	3, −53, 51
Right parieto-occipital	29, −67, 31

All ERSP plots showed significant power fluctuations in theta, alpha, beta, and gamma bands, but the most prominent power fluctuations were in the parietal and sensorimotor clusters (Fig. 5). In the left and right parieto-occipital clusters, broadband desynchronization occurred before the hit event in the rally and return conditions only. For serve hits, we observed beta synchronization and theta desynchronization in that same period. Beta desynchronization after the hit event occurred in both left and right parieto-occipital clusters for the serve and return hits but not for rally hits. In the cuneus cluster, we observed gamma synchronization before serve hits and gamma desynchronization before rally and return hits. We also found a common pattern of theta and alpha desynchronization before the hit event, followed by theta and alpha synchronization after the hit event, across all conditions in the cuneus cluster.

In the left sensorimotor cortex, the most prominent spectral power fluctuations occurred in the beta band (13–30 Hz) across conditions (Fig. 5). We observed beta desynchronization just before and around the hit event (*time 0*). Although the beta desynchronization during the rally condition was more focused around the hit event. Notably, the beta synchronization (beta rebound) after hits was strongest during a rally. There was also a significant beta rebound around 600 ms after a return. However, there was no significant beta rebound after a serve in the left sensorimotor cortex.

There were significant spectral power fluctuations in theta (3–8 Hz) and gamma (30–100 Hz) bands in the left sensorimotor cortex across hit types (Fig. 5). The serve condition showed gamma synchronization before and following the hit event whereas the rally and return conditions showed gamma desynchronization. The serve showed theta desynchronization before contacting the ball, and the rally and return hits showed more theta synchronization around the hit event within those conditions. The significant difference between serve and rally and between serve and return conditions was in the beta and gamma bands.

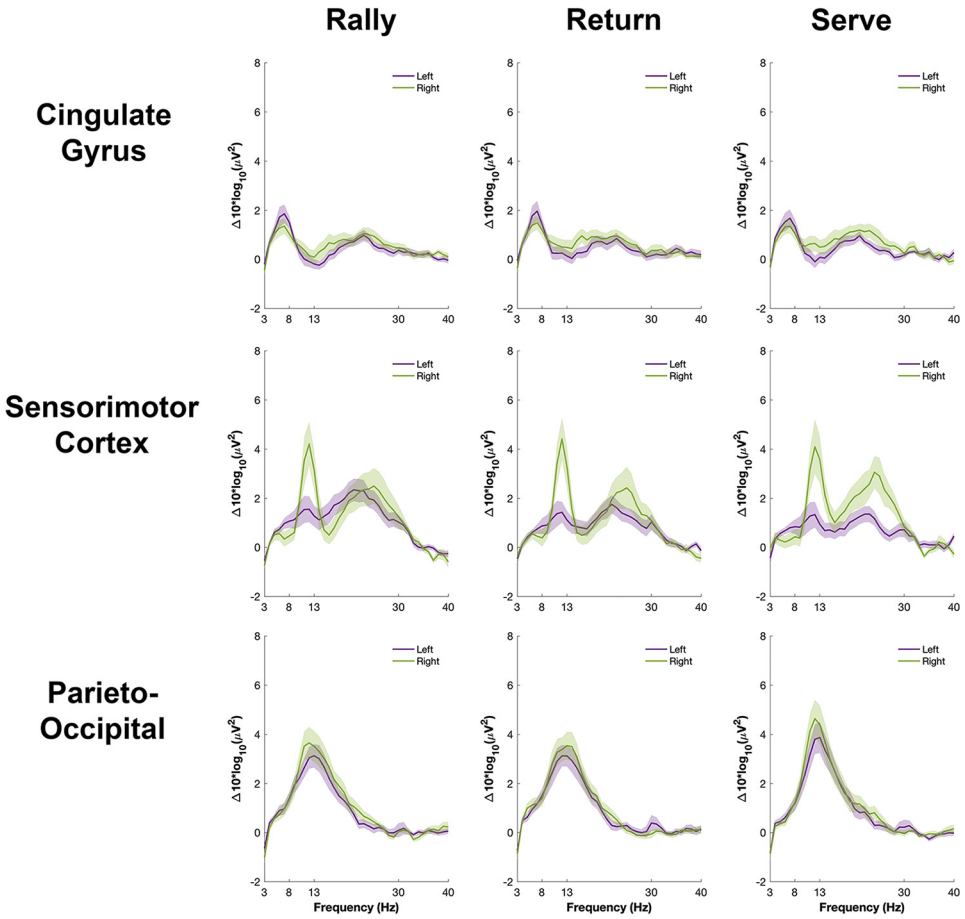

Figure 3. Power spectral density plots of the source-localized brain clusters (component-level). Average ± standard error for the left hemisphere (purple) and right hemisphere (green) in each of the corresponding brain areas (rows) for each of the following hit types (columns). The flattened spectra were calculated by taking the difference between the original power spectra and the aperiodic components (modeled with FOOOF).

The right sensorimotor cortex showed different patterns of spectral power fluctuations than the left sensorimotor cortex across hit types (Fig. 5). In the right sensorimotor cortex, there was prominent alpha and beta synchronization after the serve, preceded by very strong alpha and beta desynchronization before ball contact (*time 0*). The serve condition also showed theta synchronization before ball contact. This was very different than the rally and return conditions that showed alpha and beta synchronization and theta desynchronization before the ball hit.

We found that all hit types in the right sensorimotor cortex had more spectral power in the alpha and beta bands than the left sensorimotor cortex across all time blocks within the epoch (Fig. 6). The significant difference between left and right sensorimotor cortex for rally hits were in the alpha band −500 to 0 ms before the hit. For return hits, alpha power was significantly greater in the right than left sensorimotor cortex −1,000 to −500 ms and 500 to 1,000 ms around the hit event, and beta power was significantly greater in the right than left sensorimotor cortex −1,000 to −500 ms before the hit event. The serve hits showed significantly more right sensorimotor cortex alpha power 500 to 1,000 ms after the hit event and significantly more beta power −500 to 1,000 ms around the hit event.

In the channel-level ERSP analysis (Supplemental Fig. S3), the alpha and beta spectral power changes were less

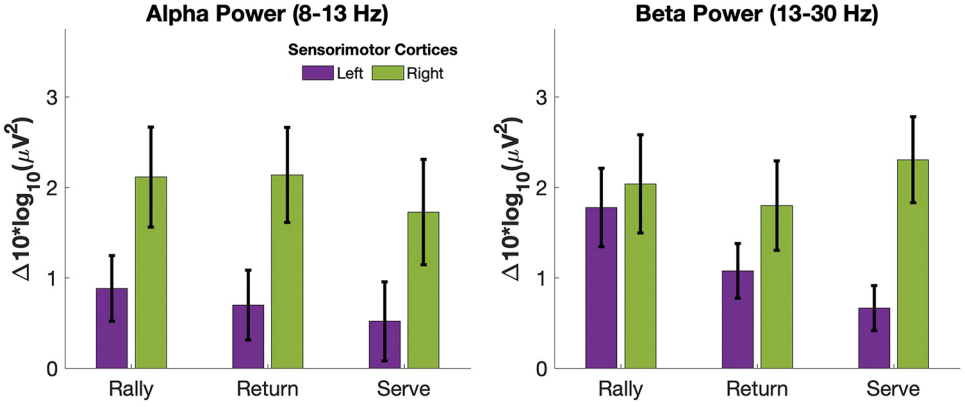

Figure 4. Means ± standard error of the sensorimotor flattened power spectra for left (purple) and right (green) clusters (only 11 participants that contributed to both clusters). *Left*: alpha/mu power (8–12 Hz). *Right*: beta power (13–30 Hz).

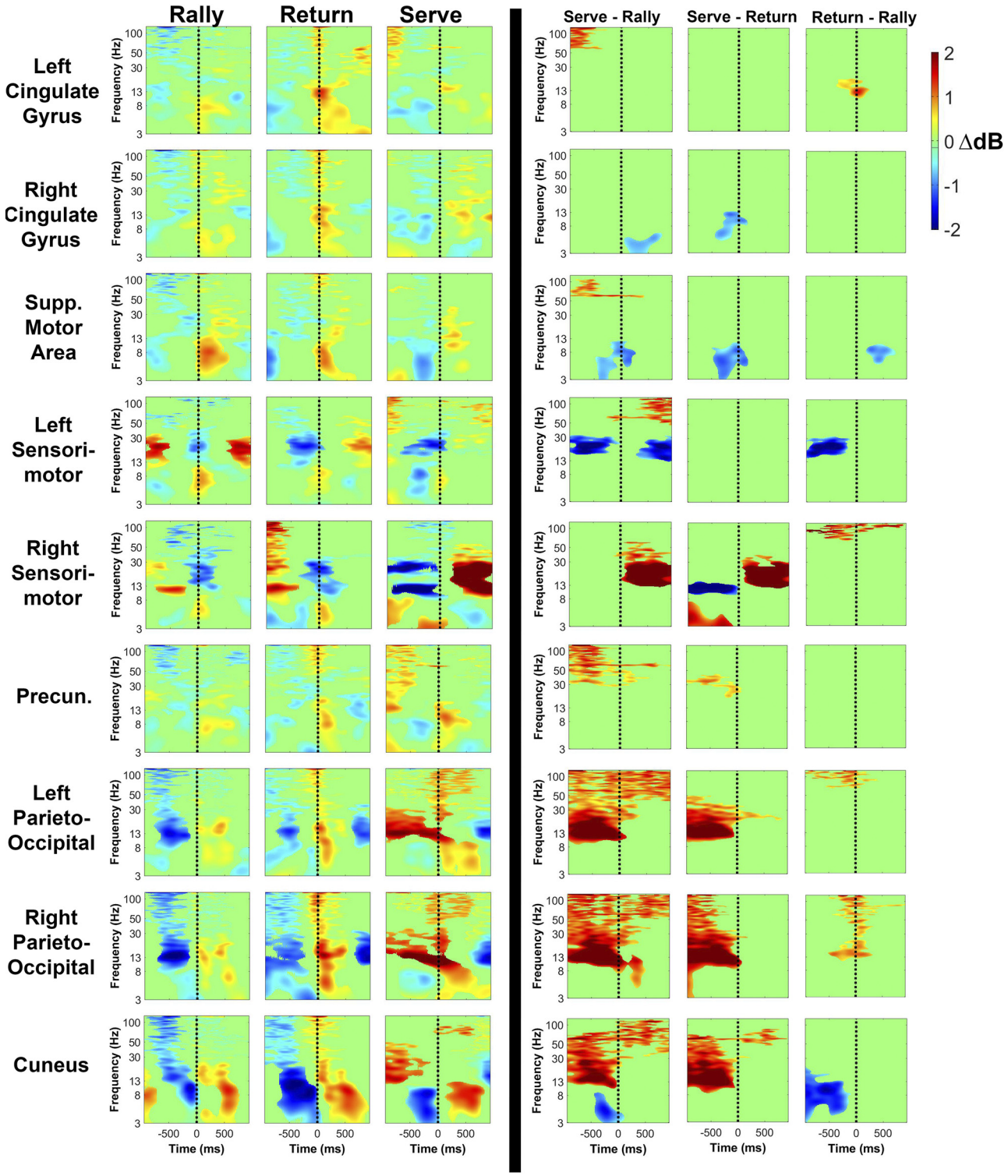

Figure 5. Event-related spectral perturbation (ERSP) plots of the group average result for rally, return, and serve hits in all clusters. Significant increases in spectral power relative to baseline are in red and significant decreases in spectral power relative to baseline are in blue ($P < 0.05$). At *time 0*, the participant hit the ball with their paddle. Spectral baseline was the average power across the entire epoch in all hit types. To the left of the bold black vertical line, the ERSPs are significance-masked within condition using bootstrap statistics. To the *right* of the bold black vertical line, the ERSPs show significant differences between hit types (permutation statistics).

pronounced and hidden by broadband power changes, as compared with the component-level ERSP analysis. However, if we focused on the alpha and beta bands, the right sensorimotor (C4 channel) had more spectral power than the left sensorimotor (C3 channel) across most of the time blocks within the epoch, similar to the component-level ERSPs.

Intertrial phase coherence (ITPC) increased in the theta (3–8 Hz) band around or just after the participant made

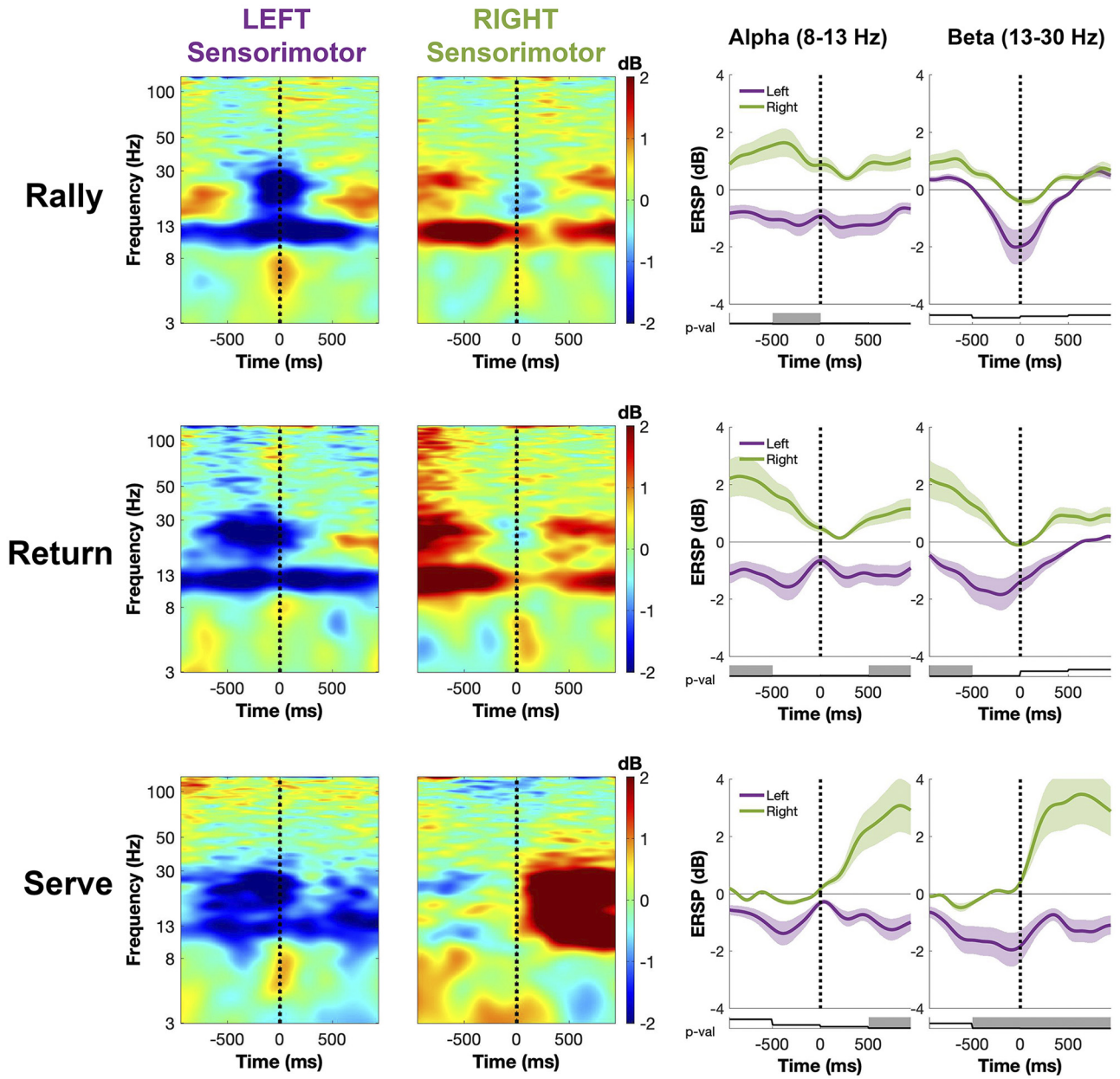

Figure 6. Event-related spectral perturbation (ERSP) plots of the left vs. right sensorimotor clusters for rally, return, and serve hits. Increases in spectral power relative to baseline are in red and decreases in spectral power relative to baseline are in blue. At *time 0*, the participant hit the ball with their paddle. Spectral baseline was the average power across the entire epoch in left and right sensorimotor clusters. The green/purple line plots show the average ± standard error of the power (relative to spectral baseline) in alpha and beta bands. The *P* value is the result of the Wilcoxon signed rank test between left and right hemispheres. Gray shading denotes significant differences in left vs. right sensorimotor ERSP power in each time block.

contact with the ball (Fig. 7). The serve hits had higher ITPC than rally hits across most clusters. The serve and return hits had similar ITPC, although it was higher for serve hits in the right cingulate and right sensorimotor cluster. Return and rally hits had similar ITPC, except for the supplementary motor area, left parieto-occipital, and right parieto-occipital clusters where the return had higher ITPC than rally hits. There were no significant differences between the left and right sensorimotor cortices in the alpha and beta bands for ITPC (Supplemental Fig. S4).

No differences in event-related coherence (ERCOH) between left and right hemispheres were found across hit types (rally vs. return vs. serve) (Fig. 8). Within hit type, there were increases in event-related coherence across the different frequencies, although there was no apparent pattern or trend. In Supplemental Fig. S5, we averaged the ERCOH across the epoch for the alpha and beta bands in the left/right sensorimotor comparison and further demonstrated little changes in coherence.

The event-related potentials time-locked to the participant hit event were very small (Supplemental Fig. S6). The unmasked cluster results were also included in the supplementary material: ERSPs in Supplemental Fig. S7 and ITPCs in Supplemental Fig. S8.

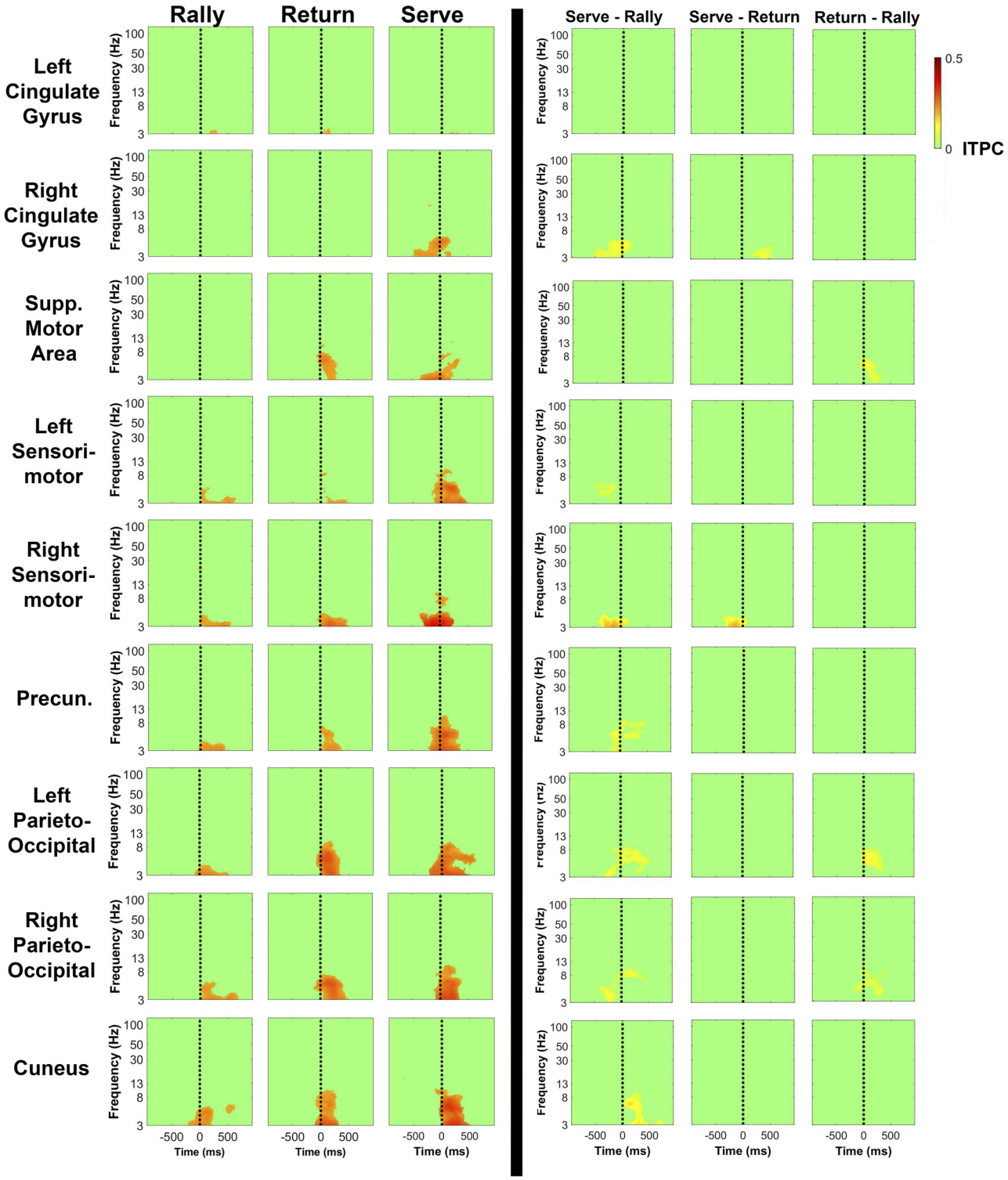

Figure 7. Intertrial phase coherence (ITPC) of the group average result for rally, return, and serve hits. Significant increases in intertrial phase coherence are in red ($P < 0.05$). At *time 0*, the participant hit the ball with their paddle. To the *left* of the bold black vertical line, the ITPC plots are significance-masked within condition using bootstrap statistics, with an additional conservative masking (any ITPC values < 0.1 are set to 0). To the *right* of the bold black vertical line, the ITPC plots show significant differences between hit types (permutation statistics, no additional conservative masking).

DISCUSSION

We found different spectral power fluctuations in the left and right sensorimotor cortices during table tennis serves, returns, and rallies. In line with our hypothesis, we found a greater magnitude of spectral power fluctuations in the right sensorimotor cortex for serve hits than return or rally hits across the entire hit epoch. Alpha/mu and beta powers

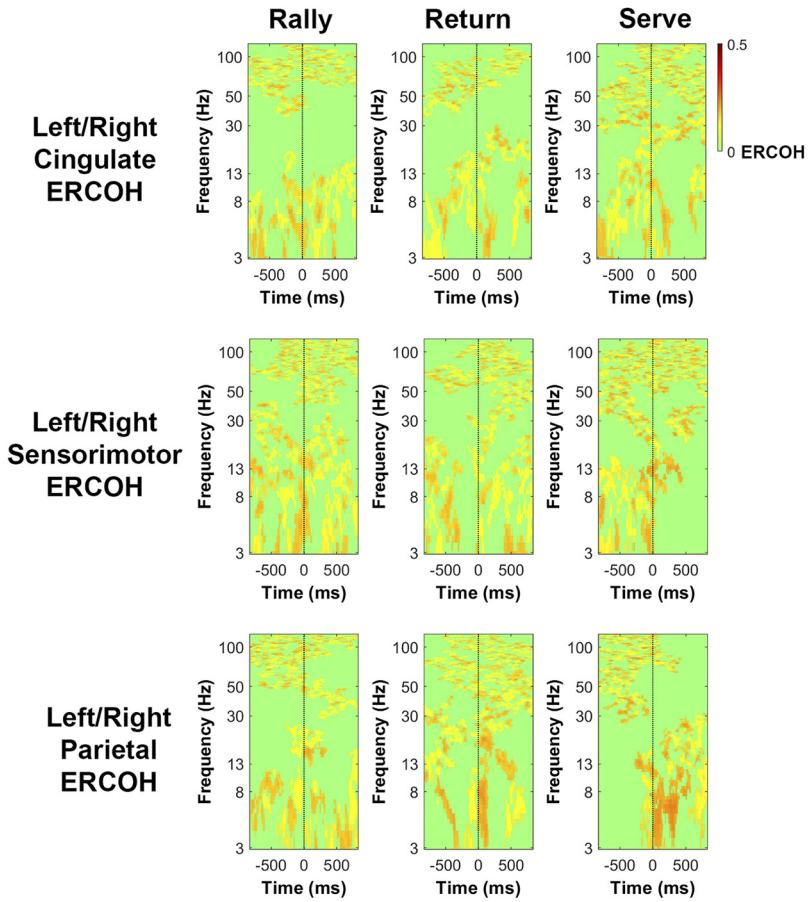

Figure 8. Event-related coherence (ERCOH) between left and right cingulate, sensorimotor, and parieto-occipital clusters for rally, return, and serve hits. Significant increases in event-related coherence are in red (within hit type condition, bootstrap statistics with $P < 0.05$). At *time 0*, the participant hit the ball with their paddle. Only the participants who contributed a component to both clusters for each pairwise comparison were chosen.

were higher in the right sensorimotor cortex compared to the left sensorimotor cortex, across the entire hit epoch. Surprisingly, we did not find any differences in interhemispheric connectivity for any of the hit types. We also found significant power fluctuations in the other brain regions, but the most prominent fluctuations were in the parieto-occipital and sensorimotor clusters.

The right sensorimotor cortex may have been more involved in serve hits than return or rally hits because of the postural control of the tossing hand. The Complementary Dominance Hypothesis developed by Sainburg et al. posits that each hemisphere is specialized for different aspects of motor control (4, 5). An example of this theory is the dynamic dominance model, which proposes that the hemisphere contralateral to the dominant side (left brain and right arm) specializes in predictive control and dynamic movement, whereas the nondominant hemisphere (right brain and left arm) specializes in endpoint precision and stability tasks. In one experiment, they had right-handed participants perform a bread-slicing motion, and they found that the right hand showed a straighter reaching performance and the left hand showed more stable holding performance in right-handed participants. This theory is in line with other studies that showed varying effects of left and right brain lesions on the different phases of an aiming movement (50, 51). In the context of a table tennis serve, both hands must work together since the paddle in the right hand must hit the ball that the left hand tossed. The serve is the only shot in the game that uses both hands to perform a coordinated bimanual maneuver, so the greater magnitude of spectral power fluctuations in the right sensorimotor cortex for serve hits may be explained by the toss.

An alternative theory that may explain the greater involvement of the right sensorimotor cortex for serve hits focuses on the type of spatial attentional mechanisms at play—global versus local. The right hemisphere is associated with encoding global features whereas the left hemisphere is associated with processing local features (52). In a concept proposed by Ivry and Roberston (53), each hemisphere is thought to encode different spatial frequencies. The right hemisphere amplifies low-frequency sensory information and the left hemisphere amplifies high frequencies. In the case of table tennis, the quick visual and sensory processing required to hit an incoming ball would require amplification of high-frequency content. The serve is less reactionary and more of a self-paced movement. A player has time to reflect and plan where and how they want to hit a serve. More visuospatial and planning processes would require the amplification of low-frequency content.

Other task- and performer-related parameters could affect hemispheric bias. The left hemisphere shows more involvement in tasks as movement complexity increases (54) and is thought to specialize in temporal processing for sequential movements. However, it is difficult to determine which table tennis shot is more "complex." On one hand, a serve is more

of a sequential, bimanual movement than rally and return hits. On the other hand, rally and return hits require faster temporal processing. Second, skill development and the novelty of a task may affect the involvement of both hemispheres. As a motor skill develops, the reliance on external sensory cues (largely represented in the right hemisphere) decreases and a consolidated internal representation of that motor skill (largely represented in the left hemisphere) increases (55). It is possible that the service motion was more novel to our participants. Many more rally hits were performed over the course of the experiment than serve hits, which could affect the internal task representation. In future studies, specific parameters of a table tennis paradigm could be systematically altered so that the task- and performer-related effects on hemispheric asymmetry could be teased apart better.

Our study complements classic hemispheric specialization research that focused on preparation during self-paced sports [e.g., golf putting (56), rifle shooting (57, 58), archery (59), etc.]. These studies found that temporal lateralization ratios indicated a shift towards right-brain dominance before movement onset, shown as a decrease in T3 (left-temporal) alpha power and a constant T4 (right-temporal) alpha power. Their findings suggested that verbal activity was inhibited just before the self-paced maneuver. A table tennis study by Wolf et al. (60) found that an imagined return of serve elicited this response but only for expert table tennis players. In our study, we similarly saw that the relative alpha power between left and right sensorimotor clusters decreased approaching the time to hit a return (Fig. 6). However, our results indicated that a decrease in the right sensorimotor alpha was more evident than any change in the left sensorimotor alpha.

We conducted our analysis at the component level, rather than the electrode level, to increase spatial resolution and resolve subtle conditional differences that are often washed out due to volume conduction (61). In our channel analysis of the alpha and beta powers over sensorimotor channels (C3 and C4), we did not find any statistical significance between hemisphere or hit types (Supplemental Figs. S1 and S2). At the component level, we found a significant difference between left and right sensorimotor clusters for both alpha and beta power (Fig. 3 and 4). There was also a notable difference in the time-frequency data between the sensorimotor components and channels (Fig. 6 vs. Supplemental Fig. S3). The channel ERSPs (Supplemental Fig. S3) had broadband increases in spectral power around the hit event, which looked very similar to muscle ERSPs for the same table tennis task (14).

We should mention a few limitations of our work. First, we did not rigorously assess the participant's handedness. All participants self-reported as being right-handed and played the game with the paddle in their right hand but evidence shows that the degree of handedness (strength) can affect measures of interhemispheric interactions (21). A future study could recruit left and right-handed people to play the game, and we could ask them to play with both dominant and nondominant hands. Second, we did not consider the effect of hitting the ball as a forehand (on the right side of the table) versus a backhand (on the left side of the table). Hemispheric specialization is modulated by spatial attention (62, 63), so this could have been a confounding factor in our analysis. In addition, other table tennis shots, besides the serve, require some degree of bimanual coordination. The serve may be the only shot that uses both hands to manipulate the ball (toss) and paddle (hit) but the other shots likely use both arms for balance during hitting. Future work could focus on different aspects of a table tennis shot in a more controlled setting. Lastly, it is important to note that readers should interpret our discussion of brain area "involvement" with caution. Drawing parallels across neuroimaging modalities remains a difficult task – both in the type of signal acquired and the different spatial scales. In this study, we reasoned that an increase in the magnitude of spectral power fluctuations in the source-localized clusters of the EEG data equates to more involvement in that brain area (19). However, it is also important to point out that EEG has lower spatial resolution than other modalities like fMRI. We reported the cluster centroid locations and their corresponding MNI coordinates (Fig. 2 and Table 1) but individual participant's components cross over different neighboring regions and likely represent a broader local network of activity. As a field, more work should use cross-modal recordings (e.g., combined EEG and fMRI).

Our findings contribute to the basic science understanding of hemispheric specialization in a natural environment. With any real-world paradigm, scientists must find a delicate balance between experimental control and ecological validity. Studying the visuomotor control of table tennis serve could provide valuable insights into the neural mechanisms underlying the execution and control of complex, self-paced movements. However, there are many theories and factors that may explain the observed left-right brain differences. Future work could look at the directional flow of information (i.e., effective connectivity) between different brain regions, as well as the brain's response during performance monitoring while controlling for skill level, to paint a better picture of what goes on inside the head of a table tennis athlete.

DATA AVAILABILITY

Source data for this study are openly available at doi.org/10.18112/openneuro.ds004505.v1.0.4.

SUPPLEMENTAL DATA

Supplemental Fig. S1, https://doi.org/10.6084/m9.figshare.23751534.

Supplemental Fig. S2, https://doi.org/10.6084/m9.figshare.23751531.

Supplemental Fig. S3, https://doi.org/10.6084/m9.figshare.23775309.

Supplemental Fig. S4, https://doi.org/10.6084/m9.figshare.23775444.

Supplemental Fig. S5, https://doi.org/10.6084/m9.figshare.23775468.

Supplemental Fig. S6, https://doi.org/10.6084/m9.figshare.23775486.

Supplemental Fig. S7, https://doi.org/10.6084/m9.figshare.23775513.

Supplemental Fig. S8, https://doi.org/10.6084/m9.figshare.23775531.

ACKNOWLEDGMENTS

The authors thank all members of the Human Neuromechanics Lab. The authors also thank to the undergraduate students who helped with data collection: Christina Collings, Corey Orlando, Sebastian Huerta, and Juan De La Espriella.

GRANTS

This research was funded by the National Science Foundation Division of Behavioral and Cognitive Sciences (BCS), Grant No. BCS-1835317 (to Daniel P. Ferris and Rachael D. Seidler).

DISCLOSURES

No conflicts of interest, financial or otherwise, are declared by the authors.

AUTHOR CONTRIBUTIONS

A.S. and D.P.F. conceived and designed research; A.S. performed experiments; A.S. and D.P.F. analyzed data; A.S., R.D.S., and D.P.F. interpreted results of experiments; A.S. prepared figures; A.S. drafted manuscript; R.D.S. and D.P.F. edited and revised manuscript; R.D.S. and D.P.F. approved final version of manuscript.

REFERENCES

1. **Knecht S**, **Dräger B**, **Deppe M**, **Bobe L**, **Lohmann H**, **Flöel A**, **Ringelstein EB**, **Henningsen H.** Handedness and hemispheric language dominance in healthy humans. *Brain* 123: 2512–2518, 2000. doi:10.1093/brain/123.12.2512.
2. **Serrien DJ**, **Ivry RB**, **Swinnen SP.** Dynamics of hemispheric specialization and integration in the context of motor control. *Nat Rev Neurosci* 7: 160–166, 2006. doi:10.1038/nrn1849.
3. **Toga AW**, **Thompson PM.** Mapping brain asymmetry. *Nat Rev Neurosci* 4: 37–48, 2003. doi:10.1038/nrn1009.
4. **Wang J**, **Sainburg RL.** The dominant and nondominant arms are specialized for stabilizing different features of task performance. *Exp Brain Res* 178: 565–570, 2007. doi:10.1007/s00221-007-0936-x.
5. **Woytowicz EJ**, **Westlake KP**, **Whitall J**, **Sainburg RL.** Handedness results from complementary hemispheric dominance, not global hemispheric dominance: evidence from mechanically coupled bilateral movements. *J Neurophysiol* 123: 1295–1304, 2018. doi:10.1152/jn.00878.2017.
6. **Haaland KY**, **Harrington DL**, **Knight RT.** Neural representations of skilled movement. *Brain* 123: 2306–2313, 2000 [Erratum in *Brain* 124: 243–244]. doi:10.1093/brain/123.11.2306.
7. **Lee SH**, **Jin SH**, **An J.** The difference in cortical activation pattern for complex motor skills: A functional near- infrared spectroscopy study. *Sci Rep* 9: 14066, 2019. doi:10.1038/s41598-019-50644-9.
8. **Milner B.** Interhemispheric differences in the localization of psychological processes in man. *Br Med Bull* 27: 272–277, 1971. doi:10.1093/oxfordjournals.bmb.a070866.
9. **Gable PA**, **Poole BD**, **Cook MS.** Asymmetrical hemisphere activation enhances global–local processing. *Brain Cogn* 83: 337–341, 2013. doi:10.1016/j.bandc.2013.09.012.
10. **Schumacher EH**, **Elston PA**, **D'Esposito M.** Neural evidence for representation-specific response selection. *J Cogn Neurosci* 15: 1111–1121, 2003. doi:10.1162/089892903322598085.
11. **Brantley JA**, **Luu TP**, **Nakagome S**, **Zhu F**, **Contreras-Vidal JL.** Full body mobile brain-body imaging data during unconstrained locomotion on stairs, ramps, and level ground. *Sci Data* 5: 180133, 2018. doi:10.1038/sdata.2018.133.
12. **Jungnickel E**, **Gehrke L**, **Klug M**, **Gramann K.** MoBI—mobile brain/body imaging. In: *Neuroergonomics: The Brain at Work and in Everyday Life*, edited by Ayaz H, Dehais F. London: Academic Press, 2019, p. 59–63.
13. **Nordin AD**, **Hairston WD**, **Ferris DP.** Human electrocortical dynamics while stepping over obstacles. *Sci Rep* 9: 4693, 2019. doi:10.1038/s41598-019-41131-2.
14. **Studnicki A**, **Downey RJ**, **Ferris DP.** Characterizing and removing artifacts using dual-layer EEG during table tennis. *Sensors (Basel)* 22: 5867, 2022. doi:10.3390/S22155867.
15. **Sørensen V**, **Ingvaldsen RP**, **Whiting HTA.** The application of co-ordination dynamics to the analysis of discrete movements using table-tennis as a paradigm skill. *Biol Cybern* 85: 27–38, 2001. doi:10.1007/PL00007994.
16. **Chettouf S**, **Rueda-Delgado LM**, **de Vries R**, **Ritter P**, **Daffertshofer A.** Are unimanual movements bilateral? *Neurosci Biobehav Rev* 113: 39–50, 2020. doi:10.1016/j.neubiorev.2020.03.002.
17. **Heinrichs-Graham E**, **Kurz MJ**, **Gehringer JE**, **Wilson TW.** The functional role of post-movement beta oscillations in motor termination. *Brain Struct Funct* 222: 3075–3086, 2017. doi:10.1007/s00429-017-1387-1.
18. **Pfurtscheller G**, **Lopes da Silva FH.** Event-related EEG/MEG synchronization and desynchronization: basic principles. *Clin Neurophysiol* 110: 1842–1857, 1999. doi:10.1016/S1388-2457(99)00141-8.
19. **Peterson SM**, **Ferris DP.** Differentiation in theta and beta electrocortical activity between visual and physical perturbations to walking and standing balance. *eNeuro* 5: ENEURO.0207-18.2018, 2018. doi:10.1523/ENEURO.0207-18.2018.
20. **Pfurtscheller G**, **Neuper C**, **Flotzinger D**, **Pregenzer M.** EEG-based discrimination between imagination of right and left hand movement. *Electroencephalogr Clin Neurophysiol* 103: 642–651, 1997. doi:10.1016/S0013-4694(97)00080-1.
21. **Bernard JA**, **Taylor SF**, **Seidler RD.** Handedness, dexterity, and motor cortical representations. *J Neurophysiol* 105: 88–99, 2011. doi:10.1152/jn.00512.2010.
22. **Fling BW**, **Walsh CM**, **Bangert AS**, **Reuter-Lorenz PA**, **Welsh RC**, **Seidler RD.** Differential callosal contributions to bimanual control in young and older adults. *J Cogn Neurosci* 23: 2171–2185, 2011. doi:10.1162/jocn.2010.21600.
23. **Fling BW**, **Seidler RD.** Fundamental differences in callosal structure, neurophysiologic function, and bimanual control in young and older adults. *Cereb Cortex* 22: 2643–2652, 2012. doi:10.1093/cercor/bhr349.
24. **Reuter-Lorenz PA**, **Stanczak L**, **Miller AC.** Neural recruitment and cognitive aging: two hemispheres are better than one, especially as you age. *Psychol Sci* 10: 494–500, 1999. doi:10.1111/1467-9280.00195.
25. **Rueda-Delgado LM**, **Solesio-Jofre E**, **Serrien DJ**, **Mantini D**, **Daffertshofer A**, **Swinnen SP.** Understanding bimanual coordination across small time scales from an electrophysiological perspective. *Neurosci Biobehav Rev* 47: 614–635, 2014. doi:10.1016/j.neubiorev.2014.10.003.
26. **Serrien DJ**, **Sovijärvi-Spapé MM.** Hemispheric asymmetries and the control of motor sequences. *Behav Brain Res* 283: 30–36, 2015. doi:10.1016/j.bbr.2015.01.021.
27. **Shim JK**, **Kim SW**, **Oh SJ**, **Kang N**, **Zatsiorsky VM**, **Latash ML.** Plastic changes in interhemispheric inhibition with practice of a two-hand force production task: a transcranial magnetic stimulation study. *Neurosci Lett* 374: 104–108, 2005. doi:10.1016/j.neulet.2004.10.034.
28. **Van Hoornweder S**, **Mora DAB**, **Depestele S**, **Frieske J**, **van Dun K**, **Cuypers K**, **Verstraelen S**, **Meesen R.** Age and interlimb coordination complexity modulate oscillatory spectral dynamics and large-scale functional connectivity. *Neuroscience* 496: 1–15, 2022. doi:10.1016/j.neuroscience.2022.06.008.
29. **Gerloff C**, **Andres FG.** Bimanual coordination and interhemispheric interaction. *Acta Psychol (Amst)* 110: 161–186, 2002. doi:10.1016/S0001-6918(02)00032-X.
30. **Verstynen T**, **Diedrichsen J**, **Albert N**, **Aparicio P**, **Ivry RB.** Ipsilateral motor cortex activity during unimanual hand movements relates to task complexity. *J Neurophysiol* 93: 1209–1222, 2005. doi:10.1152/jn.00720.2004.
31. **Nordin AD**, **Hairston WD**, **Ferris DP.** Dual-electrode motion artifact cancellation for mobile electroencephalography. *J Neural Eng* 15: 056024, 2018. doi:10.1088/1741-2552/AAD7D7.
32. **Mullen T.** *CleanLine EEGLAB Plugin*. San Diego, CA: Neuroimaging Informatics Toolsand Resources Clearinghouse (NITRC), 2012.

33. **Downey RJ**, **Ferris DP.** The iCanClean algorithm: how to remove artifacts using reference noise recordings (Preprint). arXiv 2201.11798, 2022. doi:10.48550/arXiv.2201.11798.
34. **Gonsisko CB**, **Ferris DP**, **Downey RJ.** iCanClean improves independent component analysis of mobile brain imaging with EEG. *Sensors* 23: 928, 2023. doi:10.3390/s23020928.
35. **Delorme A**, **Palmer J**, **Onton J**, **Oostenveld R**, **Makeig S.** Independent EEG sources are dipolar. *PLoS One* 7: e30135, 2012. doi:10.1371/JOURNAL.PONE.0030135.
36. **Palmer JA**, **Kreutz-Delgado K**, **Makeig S.** Super-Gaussian mixture source model for ICA. *Lect Notes Comput Sci* 3889: 854–861, 2006. doi:10.1007/11679363_106.
37. **Palmer JA**, **Makeig S**, **Kreutz-Delgado K**, **Rao BD.** *Newton method for the ICA mixture model. 2008 IEEE International Conference on Acoustics, Speech and Signal Processing*, Las Vegas, NV, 2008, p. 1805–1808. doi:10.1109/ICASSP.2008.4517982.
38. **Vorwerk J**, **Oostenveld R**, **Piastra MC**, **Magyari L**, **Wolters CH.** The FieldTrip-SimBio pipeline for EEG forward solutions. *Biomed Eng Online* 17: 37, 2018. doi:10.1186/S12938-018-0463-Y/FIGURES/8.
39. **Vorwerk J**, **Aydin Ü**, **Wolters CH**, **Butson CR.** Influence of head tissue conductivity uncertainties on EEG dipole reconstruction. *Front Neurosci* 13: 531, 2019. doi:10.3389/FNINS.2019.00531/BIBTEX.
40. **Oostenveld R**, **Oostendorp TF.** Validating the boundary element method for forward and inverse EEG computations in the presence of a hole in the skull. *Hum Brain Mapp* 17: 179–192, 2002. doi:10.1002/HBM.10061.
41. **Klug M**, **Gramann K.** Identifying key factors for improving ICA-based decomposition of EEG data in mobile and stationary experiments. *Eur J Neurosci* 54: 8406–8420, 2020. doi:10.1111/EJN.14992.
42. **Pion-Tonachini L**, **Kreutz-Delgado K**, **Makeig S.** ICLabel: an automated electroencephalographic independent component classifier, dataset, and website. *NeuroImage* 198: 181–197, 2019. doi:10.1016/J.NEUROIMAGE.2019.05.026.
43. **Rousseeuw PJ.** Silhouettes: A graphical aid to the interpretation and validation of cluster analysis. *J Comput Appl Math* 20: 53–65, 1987. doi:10.1016/0377-0427(87)90125-7.
44. **Benjamini Y**, **Hochberg Y.** Controlling the false discovery rate: a practical and powerful approach to multiple testing. *J R Stat Soc Ser* 57: 289–300, 1995. doi:10.1111/j.2517-6161.1995.tb02031.x.
45. **Cohen MX.** *Analyzing Neural Time Series Data: Theory and Practice*. Cambridge, MA: MIT Press, 2014.
46. **van Diepen RM**, **Mazaheri A.** The caveats of observing inter-trial phase-coherence in cognitive neuroscience. *Sci Rep* 8: 2990, 2018. doi:10.1038/s41598-018-20423-z.
47. **Delorme A**, **Makeig S.** EEGLAB: an open source toolbox for analysis of single-trial EEG dynamics including independent component analysis. *J Neurosci Methods* 134: 9–21, 2004. doi:10.1016/J.JNEUMETH.2003.10.009.
48. **Pernet CR**, **Appelhoff S**, **Gorgolewski KJ**, **Flandin G**, **Phillips C**, **Delorme A**, **Oostenveld R.** EEG-BIDS, an extension to the brain imaging data structure for electroencephalography. *Sci Data* 6: 103, 2019. doi:10.1038/s41597-019-0104-8.
49. **Gorgolewski KJ**, **Auer T**, **Calhoun VD**, **Craddock RC**, **Das S**, **Duff EP**, **Flandin G**, **Ghosh SS**, **Glatard T**, **Halchenko YO**, **Handwerker DA**, **Hanke M**, **Keator D**, **Li X**, **Michael Z**, **Maumet C**, **Nichols BN**, **Nichols TE**, **Pellman J**, **Poline J-B**, **Rokem A**, **Schaefer G**, **Sochat V**, **Triplett W**, **Turner JA**, **Varoquaux G**, **Poldrack RA.** The brain imaging data structure, a format for organizing and describing outputs of neuroimaging experiments. *Sci Data* 3: 160044, 2016. doi:10.1038/sdata.2016.44.
50. **Mani S**, **Mutha PK**, **Przybyla A**, **Haaland KY**, **Good DC**, **Sainburg RL.** Contralesional motor deficits after unilateral stroke reflect hemisphere-specific control mechanisms. *Brain* 136: 1288–1303, 2013. doi:10.1093/brain/aws283.
51. **Winstein CJ**, **Pohl PS.** Effects of unilateral brain damage on the control of goal-directed hand movements. *Exp Brain Res* 105: 163–174, 1995. doi:10.1007/BF00242191.
52. **Sergent J.** The cerebral balance of power: confrontation or cooperation? *J Exp Psychol Hum Percept Perform* 8: 253–272, 1982. doi:10.1037//0096-1523.8.2.253.
53. **Ivry R**, **Robertson LC.** *The Two Sides of Perception*. Cambridge, MA: MIT Press, 1997.
54. **Haaland KY**, **Elsinger CL**, **Mayer AR**, **Durgerian S**, **Rao SM.** Motor sequence complexity and performing hand produce differential patterns of hemispheric lateralization. *J Cogn Neurosci* 16: 621–636, 2004. doi:10.1162/089892904323057344.
55. **Puttemans V**, **Wenderoth N**, **Swinnen SP.** Changes in brain activation during the acquisition of a multifrequency bimanual coordination task: from the cognitive stage to advanced levels of automaticity. *J Neurosci* 25: 4270–4278, 2005. doi:10.1523/JNEUROSCI.3866-04.2005.
56. **Crews DJ**, **Landers DM.** Electroencephalographic measures of attentional patterns prior to the golf putt. *Med Sci Sports Exerc* 25: 116–126, 1993. doi:10.1249/00005768-199301000-00016.
57. **Hatfield BD**, **Landers DM**, **Ray WJ.** Cognitive processes during self-paced motor performance: An electroencephalographic profile of skilled marksmen. *J Sport Psychol* 6: 42–59, 1984. doi:10.1123/jsp.6.1.42.
58. **Hatfield BD**, **Landers DM**, **Ray WJ.** Cardiovascular-CNS interactions during a self-paced, intentional attentive state: elite marksmanship performance. *Psychophysiology* 24: 542–549, 1987. doi:10.1111/j.1469-8986.1987.tb00335.x.
59. **Salazar W**, **Landers DM**, **Petruzzello SJ**, **Han M**, **Crews DJ**, **Kubitz KA.** Hemispheric asymmetry, cardiac response, and performance in elite archers. *Res Q Exerc Sport* 61: 351–359, 1990. doi:10.1080/02701367.1990.10607499.
60. **Wolf S**, **Brölz E**, **Keune PM**, **Wesa B**, **Hautzinger M**, **Birbaumer N**, **Strehl U.** Motor skill failure or flow-experience? Functional brain asymmetry and brain connectivity in elite and amateur table tennis players. *Biol Psychol* 105: 95–105, 2015. doi:10.1016/j.biopsycho.2015.01.007.
61. **Onton J**, **Westerfield M**, **Townsend J**, **Makeig S.** Imaging human EEG dynamics using independent component analysis. *Neurosci Biobehav Rev* 30: 808–822, 2006. doi:10.1016/J.NEUBIOREV.2006.06.007.
62. **Sauseng P**, **Klimesch W**, **Stadler W**, **Schabus M**, **Doppelmayr M**, **Hanslmayr S**, **Gruber WR**, **Birbaumer N.** A shift of visual spatial attention is selectively associated with human EEG alpha activity. *Eur J Neurosci* 22: 2917–2926, 2005. doi:10.1111/j.1460-9568.2005.04482.x.
63. **Silver MA**, **Ress D**, **Heeger DJ.** Topographic maps of visual spatial attention in human parietal cortex. *J Neurophysiol* 94: 1358–1371, 2005 [Erratum in *J Neurophysiol* 95: 1291, 2006]. doi:10.1152/jn.01316.2004.